JOURNAL OF PROPULSION AND POWER
Vol. 25, No. 2, March–April 2009

Combustion-Noise Characterization of a Turbofan Engine with a Spectral Estimation Method

Daniel Blacodon*
ONERA, 92322 Châtillon, France

DOI: 10.2514/1.37013

A full-scale test on a turbofan engine has been carried out in the framework of a European project to assess the acoustic benefits of new exhausts and novel hot-stream streamliners in the reduction of the overall jet noise level radiated in the far field. The purpose of the tests is also to provide a better understanding of combustion noise, which is one of the main issues for turbofan engines because of the significant noise reduction obtained for other acoustic sources such as the fan and jet by using innovative efficient silencers and acoustics liners. This work investigates the use of the so-called spectral estimation method to separate the combustion noise from other noise sources measured with a near-field array of microphones. The comparisons between the estimated and measured spectra downstream, at the location at which the combustion noise is dominant, yield promising results, suggesting that the procedure of discrimination is relevant.

Nomenclature

A_i	=	actual power level for monopole i
$\hat{A}_i$	=	estimated power level for monopole i
$\hat{A}_i^l$	=	estimated power level for monopole i belonging to the source subregion l
C_{noise}	=	combustion noise estimated with the spectral estimation method
f	=	frequency, Hz
G_{ni}	=	Green function for a spherical wave radiating from focus point i to microphone n ($e^{jkR_{ni}}/R_{ni}$)
J	=	number of monopole sources distributed in the 20 source subregions
J_{noise}	=	jet noise estimated with the spectral estimation method on M_{40}
k	=	acoustic wave number
L	=	number of subregions use to estimate combustion noise
Lc	=	length of the emission region of combustion noise
M_{40}	=	microphone of the array located downstream at the angular location of 123 deg
N	=	number of monopole sources distributed in each of the 20 source subregions
O_{noise}	=	overall noise estimated at the engine exhaust estimated with the spectral estimation method on M_{40}
P_n^l	=	estimated levels on microphone n due to the subregion l
R_{ni}	=	distance between the monopole i and the microphone n
$[\Gamma^{\text{mes}}(f)]$	=	cross-spectral matrix resulting from the acoustic measurements
$\Gamma_{m,n}^{\text{mes}}(f)$	=	cross-power spectrum between the measured signals with microphones m and n
$[\Gamma^{\text{mod}}(f)]$	=	cross-spectral matrix obtained with the model
$\Gamma_{m,n}^{\text{mod}}$	=	cross-power spectrum between the mth and nth model signals
Δf	=	frequency resolution, Hz
Δx	=	sampling interval on the x axis
Δy	=	sampling interval on the y axis
*	=	complex conjugation

Presented as Paper 2940 at the 14th AIAA/CEAS Aeroacoustics Conference, Vancouver, Canada, 5 May–5 July 2008; received 5 February 2008; revision received 20 Sept. 2008; accepted for publication 8 October 2008.

*Research Engineer, Computational Fluid Dynamics and Aeroacoustics Department; Daniel.Blacodon@onera.fr.

I. Introduction

IN THE framework of a European project, a full-scale test on a turbofan engine was carried out during the last quarter of 2006. One of the primary objectives of the experiment was to assess the acoustic benefits of new exhausts and novel hot-stream streamliners in the reduction of the overall jet noise level radiated in the far field. Combustion noise was studied more particularly because it now appears to be a major contributor to the in-flight noise of an aircraft, because the acoustic nuisance from the other noise sources such as the fan and jet has been reduced by the use of innovative efficient silencers and acoustics liners.

This study is focused on the separation of combustion noise from acoustic measurements performed in the near field with an array of microphones. This is a complex problem to solve because a turbofan engine simultaneously radiates fan, compressor, turbine, jet, and combustion noise that can generate both broadband and narrowband noise in the same frequency range.

One way of overcoming this difficulty is to take two local measurements in the engine core to extract the characteristics of combustion noise from the spectrum measured in the far field [1–3]. The methods based on this solution, often named the three-sensor method (TSM), are very easy to implement, because they only require the computation of the cross-power spectra between the three signals considered previously. However, even though the TSM provides the actual contributions of internal noise sources emitted in the far field compared with the classical cross spectrum, which trends to give an underestimate [4], the delicate machining inside the engine to install the two probes limits its use in practice.

In recent years, more attention has been devoted to development and use of methods based on phased-array measurements to investigate the core noise. A number of papers [5,6] deal with the characterization of the noise-source distribution along the jet axis that contributes to the overall far-field noise using the classical beamforming (CBF). The information provided by CBF increases our understanding of combustion noise but is not completely suitable for evaluating the parameters that influence the spectral content and the levels of combustion noise exactly.

Today, there is some interest in using diagnostic tools based on array measurements that can characterize the acoustic sources of interest in level and frequency. Miles [7] has proposed an interesting approach based on the separation of correlated and uncorrelated noise sources from far-field measurements. The discrimination procedure consists of finding the parameters of a model combining coherent and incoherent noise sources such that the estimated auto- and cross spectra best fit the measured ones. The results presented by the author have shown that the method is suitable for identifying and ranking combustion noise at low frequencies.

More recently, the use of coherent source model has been considered in [8] with the so-called DAMAS-C method. A large number of potential applications could be covered using this innovative method, even if it has only been validated in the characterization of airframe noise at present.

In this study, we propose to extract combustion noise from the near-field measurements using the so-called spectral estimation method (SEM) [9]. This method was developed to characterize compact and extended acoustic sources into levels and has been successfully applied in tests involving airframe noise [10]. However, the question that we must attempt to answer is whether we can characterize combustion noise using a model of uncorrelated monopole sources such as the one considered in SEM. The results presented in this paper intend to provide an answer to this question.

II. Analysis Method

In this study, the procedure for separating combustion noise from the other noise sources radiated at the engine exhaust is based on a priori knowledge of this particular component of noise and on assumptions that we hope will be relevant a posteriori. These are illustrated in Fig. 1 and can be explained as follows:

1) At very low operating conditions, the noise source radiated at the engine exhaust, downstream at the angular direction of around 123 deg, is mainly due to combustion noise.

2) The combustion noise always emits from the same restricted region of an unknown length Lc, and it is assumed that this region is separated from the other source regions in the jet.

It is obvious from the previous discussions that the length Lc is the only unknown that has to be estimated to solve the problem of separation of the acoustic sources. The strategy considered hereafter to estimate Lc consists of splitting the zone of the jet located between the output section of the nozzle up to ten diameters of section (i.e., from $x = 0$ up to 10 m) into 20 subregions of the same dimensions. Those, set arbitrarily, have a 0.5 m length on the x axis and a width of 40 cm on the y axis. Then J uncorrelated monopole sources with unknown amplitudes are distributed in the 20 subregions (Fig. 2).

Finally, we define a model cross-power spectrum $\Gamma^{\text{mod}}_{m,n}(f)$ between the output signals of the mth and nth microphones of the array, which would be due to the radiation of the virtual monopole sources impinging on the microphones. $\Gamma^{\text{mod}}_{m,n}(f)$ has the following form:

$$\Gamma^{\text{mod}}_{m,n}(f) = \sum_{i=1}^{J} G_{mi} A_i(f) G^*_{ni} \tag{1}$$

The basic separation procedure carried out with SEM consists of performing the three following steps:

1) Estimate the powers levels $A_i(f)$ of the monopole sources J by minimizing the mean squared error between the array $[\Gamma^{\text{mes}}(f)]$ and model $[\Gamma^{\text{mod}}(f)]$ cross-spectral matrices under a positivity constraint to ensure that positive solutions $\hat{A}_i(f)$ $(i = 1, 2, \ldots, J)$ will be obtained.

2) Compute $P^l_{n=40}(f)$, the levels radiated by each subregion l $(l = 1, 2, \ldots, 20)$, at the location of microphone M_{40}, downstream at the angular position of 123 deg, at which the combustion noise is assumed to be dominant using the following equation:

$$P^l_{n=40}(f) = \sum_{i=1}^{N} \frac{\hat{A}^l_i(f)}{R^2_{ni}} \tag{2}$$

3) Assess the length Lc at a very low operating condition. According to assumptions 1 and 2 in Sec. II, this is equivalent to finding the number L of subregions to sum, such that the following relation is verified:

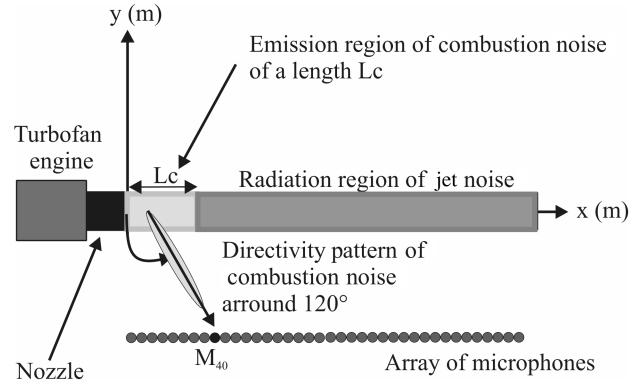

Fig. 1 Geometry of the separation problem of combustion and jet noise sources.

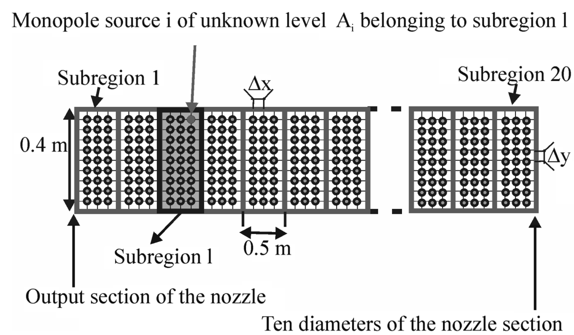

Fig. 2 Grid used to apply the procedure of noise-source separation.

$$\sum_{l=1}^{L} P^l_{n=40}(f) \cong \Gamma^{\text{mes}}_{40,40}(f) \tag{3}$$

In other words, the integrated power levels across the region located from $x = 0$ and $Lc = 0.5L$ must match the spectrum measured with microphone M_{40}. The length Lc determined in the last step will be used to characterize combustion noise generated at all of the operating conditions examined in this paper.

Finally, we may therefore express C_{noise}, the integrated power levels due to the combustion noise on M_{40}, as follows:

$$C_{\text{noise}}(f) = \sum_{l=1}^{L} P^l_{n=40}(f) \tag{4}$$

.

III. Experimental Setup and Signal Analysis

The experimental setup used during the full-scale tests carried out with the turbofan engine is shown in Fig. 3. Two nested linear subarrays composed of 70 microphones, $\frac{1}{2}$ in. 4134 Brüel&Kjaer (Fig. 4), were laid out on the ground to measure the acoustic near field radiated by the engine. The short array, with a length of 4 m, was designed with 41 microphones evenly spaced at 10 cm to measure high-frequency sources radiating from the exhausts up to the end of the potential cone of the jet. The wide array, with a length of 9.80 m, was made up of 50 microphones evenly spaced at 20 cm to measure the low-frequency noise sources emitted from the end of the potential cone, up to ten diameters of the nozzle-exit cross section.

A. Data Processing

The array of microphones was calibrated before each test using a pistonphone. The array cross-power matrix $[\Gamma^{\text{mes}}]$ needed to apply SEM was estimated using 1000 data blocks of 1024 samples each, sampled at the frequency of 31,250 Hz (i.e., $\Delta f = 31250/1024 = 30.51$ Hz). The levels of 974 virtual monopole sources required to

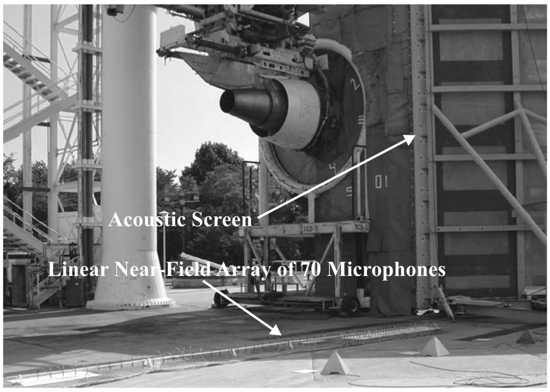

Fig. 3 Experimental setup.

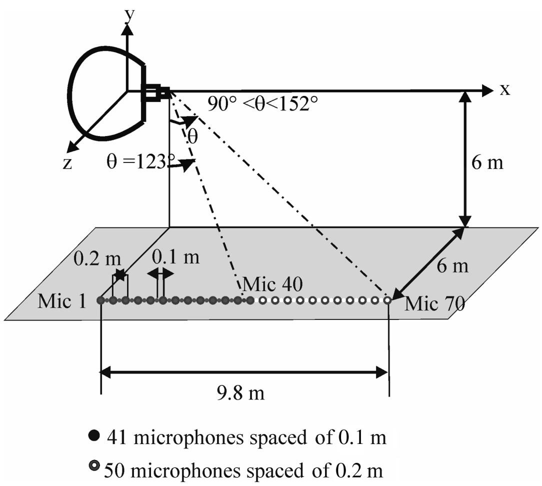

Fig. 4 Geometry and location of the two subarrays.

estimate $P^l_{n=40}(f)$ [Eq. (2)] were computed at the nodes of a grid (from $x = 0$ up to 10 m and from $y = -0.2$ up to 0.2 m), with an elementary mesh of size $\Delta s = \Delta x \Delta y$ (with $\Delta x = \Delta y = 0.05$ m) at the discrete frequencies $f_q = q\Delta f$ ($q = 1, \ldots, 163$) in the frequency range of 0 to 5 kHz.

B. Data Analysis with SEM

During the tests, five items of equipment were installed on the turbofan engine: namely, the baseline, the squid nozzle, the classical plug, the external plug, and the ceramic hollow-sphere plug. However, the present study is focused on the results obtained when the turbofan engine is equipped with the external plug, for approach flights under very low and low operating conditions and takeoff flights under high and very high operating conditions, according to Fig. 5.

1. Approach Under Very Low Operating Conditions

We start with the analysis of the data recorded during the tests under very low operating conditions, in which combustion noise is assumed to be the dominant downstream toward the angular position of 123 deg. This test was used to estimate the length Lc of the region from which combustion noise radiates. Figure 6 presents the spectrum measured with the microphone M_{40}. It appears that combustion noise radiates in the frequency range of 0 to 1600 Hz. Fan noise, which radiates above 2 kHz, is considered in this study to be a spurious noise source. Consequently, the frequency range of interest for characterizing combustion noise will be limited to 0–2 kHz for the other analysis presented in the paper.

The integrated power levels obtained with SEM for the subregions 1 to 6 are superimposed in Fig. 6 on the spectrum of M_{40}.

However, the integrated power levels for subregions 7 to 20 are not presented here, because their amplitudes are too weak compared with the levels of the spectrum measured with M_{40}. As could be foreseen, the contribution of combustion noise is more important in subregion 1 close to the output section of the nozzle than beyond subregion 5 downstream. This result suggests that combustion noise radiates from a region covering subregions 1 to 5. Therefore, we may

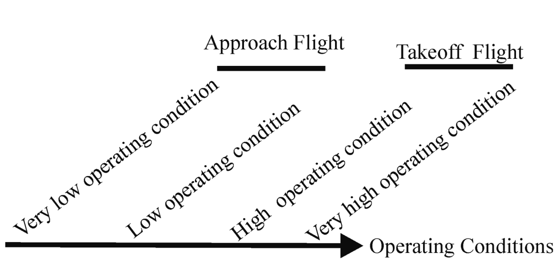

Fig. 5 Operating conditions examined in the study.

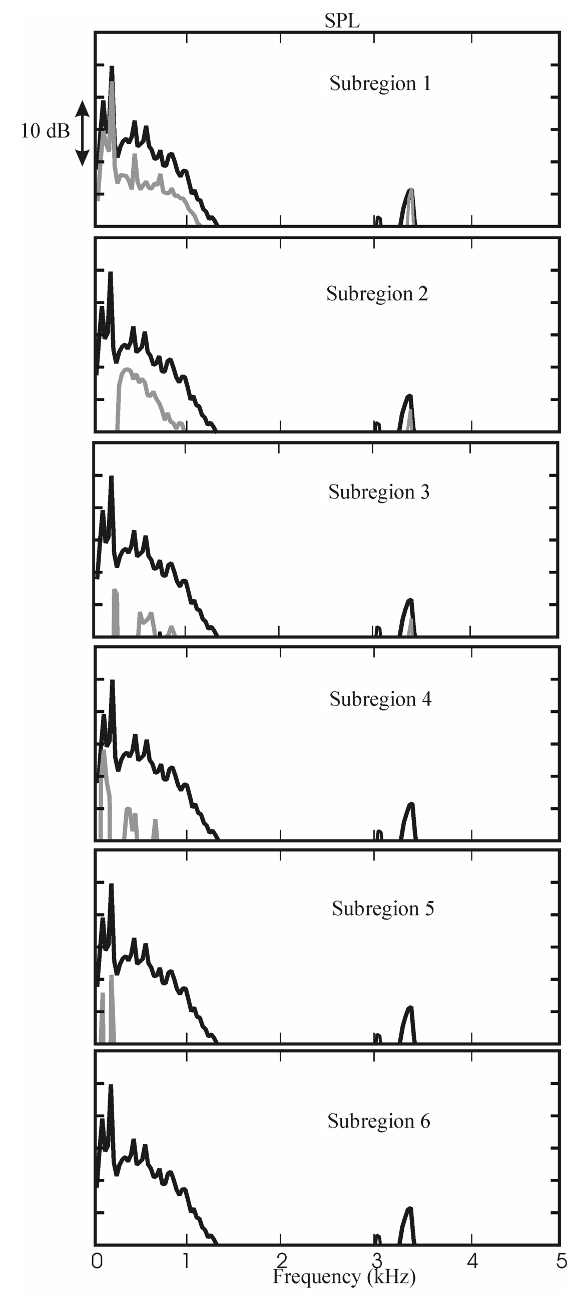

Fig. 6 Approach under very low operating conditions: comparison between the spectrum measured with M_{40} and the results obtained with SEM for the subregions 1 to 6.

consider that the length of the combustion-noise emission region is $Lc = 2.5$ m.

This result is confirmed in Fig. 7, in which C_{noise} obtained by summing the contribution of subregions 1 to 5 [$L = 5$ in Eq. (4)] matches the spectrum measured with M_{40} very well.

We have just discussed the characterization of combustion noise using data recorded with the near-field array of microphones. We should now look at whether it is possible to distinguish the contribution of other noise sources in the spectrum measured with M_{40}. At this point, we should point out that during the experiment, an acoustic barrier was used to limit acoustic pollution by the fan and compressor noise downstream. Hence, the phased array, which is located downstream, mainly measures combustion and jet noise. Thus, we deduce from this information that the other noise sources measured with the phased array are mainly due to jet noise. Therefore, the simple way to assess the contribution of jet noise, named J_{noise} here, is to estimate the integrated power levels using the following relation:

$$J_{\text{noise}}(f) = \sum_{l=N+1=6}^{20} P^{l}_{n=40}(f) \tag{5}$$

Moreover, it is also interesting to compute the integrated power levels due to overall noise sources, named O_{noise} (i.e., combustion plus jet noise), radiated on M_{40} with the following relation:

$$O_{\text{noise}}(f) = \sum_{l=1}^{20} P^{l}_{n=40}(f) \tag{6}$$

Indeed, by comparing O_{noise} and the spectrum measured with M_{40}, we can assess the accuracy of the estimation procedure described in Sec. II after Eq. (1).

Figure 8 shows that jet noise J_{noise} is weaker than combustion noise C_{noise} at the operating conditions considered here. Furthermore, it also appears that there is a very small difference between combustion noise, the spectrum measured, and O_{noise}. We can consider this result to be a validation of the procedure used to separate combustion and jet noise from the near-field measurements.

2. Approach Under Low Operating Conditions

Under these operating conditions, combustion noise C_{noise} is again dominant (Fig. 9). Its level matches the spectrum measured with M_{40}. This is also the case for O_{noise}. In contrast, the level of J_{noise} is higher than that obtained under very low operating conditions (Fig. 8), but it still remains lower than C_{noise}.

3. Takeoff Under High Operating Conditions

The results presented in Fig. 10 show that spectrum measured with M_{40} is not totally due to combustion noise. Indeed, we note that the contribution of jet noise is of the same order as that of combustion noise. There is also a small difference between the spectrum measured and O_{noise}.

4. Takeoff Under Very High Operating Conditions

In the last test considered here, we examined a takeoff at a very high power setting. Clearly, jet noise is now the dominant noise source (Fig. 11). Its level is comparable with the spectrum measured with M_{40} and with the amplitude of O_{noise}, and combustion noise is approximately 3 dB weaker.

C. Mapping of Noise Sources in the Jet with CBF

In the previous section, we presented results concerning the separation of combustion and jet noise from near-field measurements by an array of microphones. The procedure of separation with SEM is mainly based on the assumption that the length Lc of the combustion-noise emission region is independent of the operating

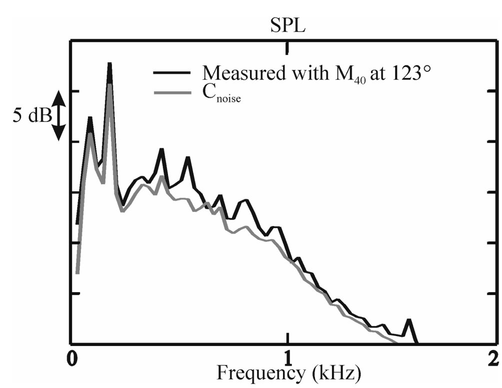

Fig. 7 Approach under very low operating conditions: comparison between the spectrum measured with M_{40} and C_{noise} obtained with SEM (SPL denotes sound pressure levels).

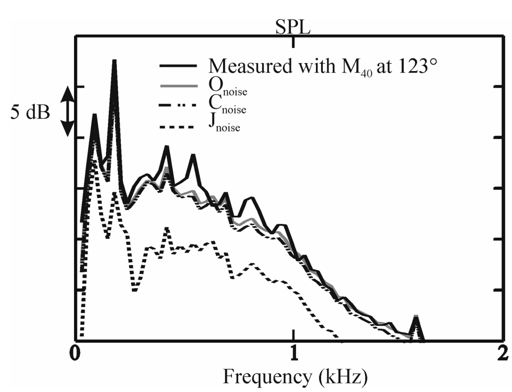

Fig. 8 Approach under very low operating conditions: comparison between the spectrum measured with M_{40}, C_{noise}, J_{noise}, and O_{noise} obtained with SEM.

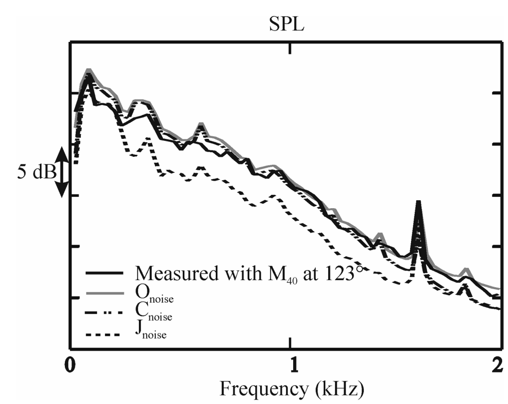

Fig. 9 Approach under low operating conditions: comparison between the spectrum measured with M_{40} and the results obtained with SEM.

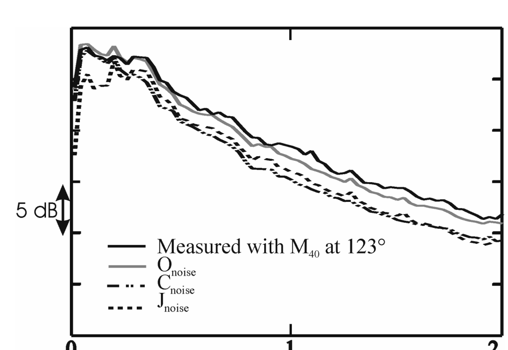

Fig. 10 Takeoff under high operating conditions: comparison between the spectrum measured with M_{40}, C_{noise}, J_{noise}, and O_{noise}.

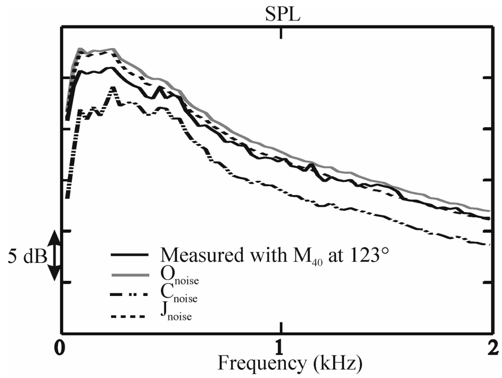

Fig. 11 Takeoff under high operating conditions: comparison between the spectrum measured with M_{40} and the results obtained with SEM.

conditions. In this section, we examine the validity of this assumption using acoustic maps computed with CBF.

All of the acoustic maps presented here are plotted for the region along the jet located from $x = 0$ to 10 m and in the frequency range of 0 to 2 kHz for the four operating conditions considered in the previous section. A dotted line is plotted on each of the maps computed with CBF to show the contribution of combustion and jet noise, respectively, located on the left part and the right part of the dotted line.

1. Approach Flight Under Very Low Operating Conditions

Figure 12 shows two narrowband sources centered around 75 and 150 Hz, located near the nozzle-exit plane. These acoustic sources have not been yet identified. They may be due to a resonance phenomenon inside the engine. In addition, we can observe a wideband source in the entire frequency band of 0 to 2 kHz. This wideband source can be attributed to combustion noise, because under these operating conditions, this is the only dominant noise source. Its space extent, deduced from Fig. 12, covers the region from $x = 0$ to 2.5 m. This result is in agreement with the conclusion obtained with SEM in Sec. III.B.1.

2. Approach Flight Under Low Operating Conditions

The results obtained in Fig. 13 are very similar to those presented in Fig. 12 for very low operating conditions, except that the two narrowband sources at 75 and 150 Hz have merged to generate a narrowband source in the frequency range of 0 to 400 Hz. Apart from that, a dominant wideband source in the range of 0 to 2 kHz appears again, which is due to combustion noise. Indeed, it presents the

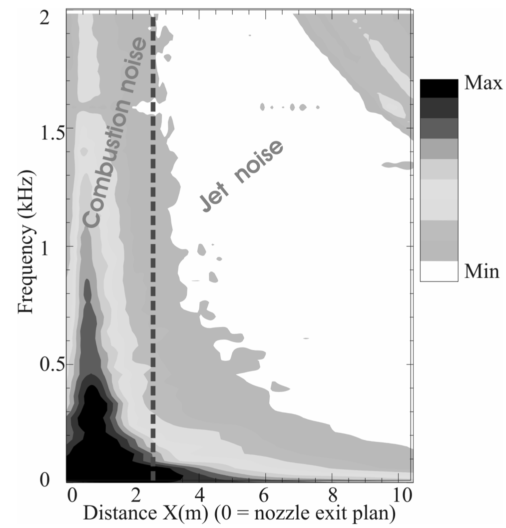

Fig. 13 Approach flight under low operating conditions: result obtained with CBF.

similar characteristics in space and frequency to the wideband source in Fig. 12, which we attributed to combustion noise. This result tends to show that the space extent and the emission frequency of combustion noise remain unchanged for two very different operating conditions. Thus, we can consider that assumption 2 made at the beginning of Sec. II is realistic.

3. Takeoff Flight Under High Operating Conditions

Again, the combustion noise radiates from $x = 0$ to 2.5 m, in the frequency range of 0 to 2 kHz (Fig. 14). The result of this test corroborates the observations made for the two previous scenarios presented in Figs. 12 and 13 obtained, respectively, under very low and low operating conditions.

Furthermore, there is a narrowband source with a high level centered on the location $x = 1$ m and at the frequency $f = 300$ Hz. Moreover, the result shows a broadband source located from $x = 2.5$ to 10 m, for which the level decreases in the downstream direction. This noise source is certainly due to jet noise and has a level of the same order as combustion noise. The observation made here is in agreement with the conclusion exposed in Sec. III.B.3. It also validates assumption 1 made at the beginning of Sec. II. In other words, under lower operating conditions, jet noise is much weaker than combustion noise. This is why jet noise does not appear in Figs. 12 and 13, respectively, obtained at approach flight under very low and low operating conditions.

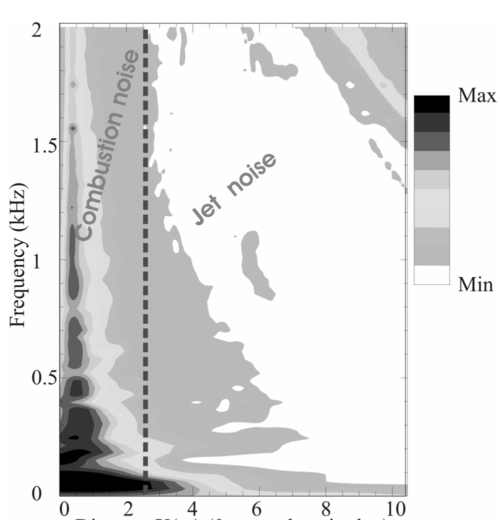

Fig. 12 Approach flight under very low operating conditions: result obtained with CBF.

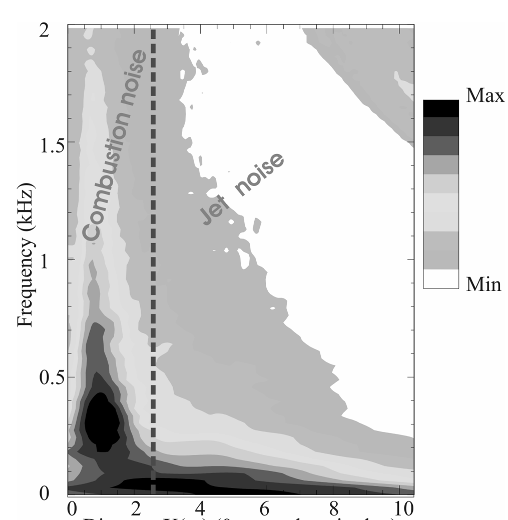

Fig. 14 Takeoff flight under high operating conditions: result obtained with CBF.

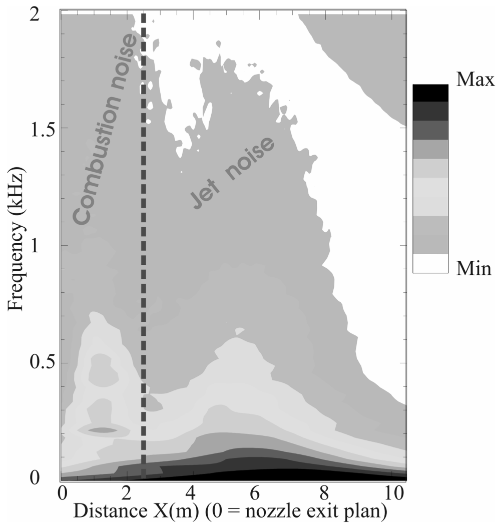

Fig. 15 Takeoff flight under very high operating conditions: result obtained with CBF.

4. Takeoff Flight Under Very High Operating Conditions

Figure 15 shows that combustion again radiates from $x = 0$ to 2.5 m, in the frequency range of 0 to 2 kHz. However, it is not the dominant noise source as in Figs. 12–14, respectively, obtained during the approach flight under very low and low operating conditions and during a takeoff flight under high operating conditions. Clearly, jet noise is located from $x = 2.5$ to 10 m. Now it is the dominant noise source radiated at the engine exhaust.

IV. Conclusions

This study has presented a methodology for separating combustion noise from jet noise based on measurements carried out with a near-field array of microphones and the spectral estimation method (SEM). This methodology involves estimating the length Lc of the region from which combustion noise radiates. Lc is estimated in the following way:

1) First, compute and propagate downstream the integrated power levels obtained for 20 source subregions in the jet at the engine exhaust, at the location of the microphone M_{40} of the array in which combustion noise is dominant,

2) Second, determine the number of subregions to sum, giving the same characteristics, both in shape and in level, to those of the spectrum measured with M_{40}.

The separation procedure was applied to data measured during a full-scale test on a turbofan engine under several operating conditions. The following observations were deduced:

1) The region from which combustion noise emanates has the same length under very low and high operating conditions.

2) Combustion noise is dominant both at the lowest and highest approach ratings and jet noise for takeoff flights taking place under very high operating conditions.

The results presented in this study using SEM, which are based on a model of uncorrelated monopole sources, appear to be relevant in the separation of combustion and jet noise. A complementary study will be carried out to refine the conclusions obtained during this study.

Acknowledgments

This work was supported by the European Community and by the Department of Numerical Simulation and Aeroacoustics of ONERA. The author would like to express his gratitude to the noise team of the high-technology Safran group for many helpful stimulating discussions on combustion noise and to the ONERA acquisition and test team. The results were obtained using a turbofan engine, and the test bench was made available by the Société Nationale d'Etude et de Construction de Moteurs d'Aviation (SNECMA).

References

[1] Shivashankara, B. N., "High Bypass Ratio Engine Noise Component Separation by Coherence Technique," *Journal of Aircraft*, Vol. 20, No. 3, 1983, pp. 236–242.
doi:10.2514/3.44858

[2] Eugene A. Krejsa, "New Technique for the Direct Measurement of Core Noise from Aircraft Engines," NASA TM-82634, 1981.

[3] Chung, J. Y., "Rejection of Flow Noise Using a Coherence Function Method," *Journal of the Acoustical Society of America*, Vol. 62, No. 2, Aug. 1977, pp. 388–395.
doi:10.1121/1.381537

[4] Guédel, A., and Farrando, A., "Experimental Study of Turboshaft Engine Core Noise," *Journal of Aircraft*, Vol. 23, No. 10, 1986, pp. 763–767.
doi:10.2514/3.45378

[5] Lee, S., "Phased-Array Measurement of Modern Regional Aircraft Turbofan Engine Noise," 12th AIAA/CEAS Aeroacoustics Conference, AIAA Paper 2006-2653, May 2006.

[6] Saligrama, R., Venkatesh, D., Polak, R., and Satish, N., "Beamforming Algorithm for Distributed Source Localization and Its Application to Jet Noise," *AIAA Journal*, Vol. 41, No. 7, 2003, pp. 1238–1246.
doi:10.2514/2.2092

[7] Miles, J., "Procedure for Separating Noise Sources In Measurements of Turbofan Engine Core Noise," 12th AIAA/CEAS Aeroacoustics Conference, Paper 2006-2580, Cambridge, MA, May 2006.

[8] Brooks, T., and Humphreys, W., "Extension of DAMAS Phased Array Processing for Spatial Coherence Determination (DAMAS-C)," 12th AIAA/CEAS Aeroacoustics Conference, AIAA Paper 2006-2654, Cambridge, MA, May 2006.

[9] Blacodon, D., and Elias, G., "Level Estimation of Extended Acoustic Sources Using a Parametric Method," *Journal of Aircraft*, Vol. 41, No. 6, 2004, pp. 1360–1369.
doi:10.2514/1.3053

[10] Blacodon, D., "Analysis of the Airframe Noise of an A320/A321 with a Parametric Method," *Journal of Aircraft*, Vol. 44, No. 1, 2007, pp. 26–34.
doi:10.2514/1.20295

K. Frendi
Associate Editor